Naval Research Laboratory

Washington, DC 20375-5320

NRL/MR/5650--14-9532

Coupled Mode Formalism: Connecting Phasor, Matrix, and Geometrical Approaches

NICHOLAS J. FRIGO

U.S. Naval Academy
Physics Department
Annapolis, Maryland

VINCENT J. URICK
FRANK BUCHOLTZ

Photonics Technology Branch
Optical Sciences Division

May 30, 2014

REPORT DOCUMENTATION PAGE

Form Approved
OMB No. 0704-0188

1. REPORT DATE *(DD-MM-YYYY)*	**2. REPORT TYPE**	**3. DATES COVERED** *(From - To)*
30-05-2014	Memorandum	01-01-2013 – 03-07-2013

4. TITLE AND SUBTITLE

Coupled Mode Formalism: Connecting Phasor, Matrix, and Geometrical Approaches

5a. CONTRACT NUMBER

5b. GRANT NUMBER

5c. PROGRAM ELEMENT NUMBER
62271N

6. AUTHOR(S)

Nicholas J. Frigo,[1] Vincent J. Urick, and Frank Bucholtz

5d. PROJECT NUMBER

5e. TASK NUMBER
EW-271-003

5f. WORK UNIT NUMBER
6582

7. PERFORMING ORGANIZATION NAME(S) AND ADDRESS(ES)

Naval Research Laboratory, Code 5650
4555 Overlook Avenue, SW
Washington, DC 20375-5320

8. PERFORMING ORGANIZATION REPORT NUMBER

NRL/MR/5650--14-9532

9. SPONSORING / MONITORING AGENCY NAME(S) AND ADDRESS(ES)

Office of Naval Research
One Liberty Center
875 North Randolph Street, Suite 1425
Arlington, VA 22203-1995

10. SPONSOR / MONITOR'S ACRONYM(S)

ONR

11. SPONSOR / MONITOR'S REPORT NUMBER(S)

12. DISTRIBUTION / AVAILABILITY STATEMENT

Approved for public release; distribution is unlimited.

13. SUPPLEMENTARY NOTES

[1]U.S. Naval Academy, Physics Department, Annapolis, MD

14. ABSTRACT

In this report, we examine the formalism of coupled mode theory from several viewpoints, using the fiber optic directional coupler as a model problem to unify the discussion. With this model, we present the basic maps and tools used in describing coupled systems, emphasizing the connections between the approaches by using a consistent notation across phasor, matix algebra, and geometrical descriptions.

15. SUBJECT TERMS

Coupled mode theory
Polarization
Fiber optics
Fiber-optic coupler

16. SECURITY CLASSIFICATION OF:			**17. LIMITATION OF ABSTRACT**	**18. NUMBER OF PAGES**	**19a. NAME OF RESPONSIBLE PERSON**
a. REPORT	**b. ABSTRACT**	**c. THIS PAGE**			Vincent J. Urick
Unclassified Unlimited	Unclassified Unlimited	Unclassified Unlimited	Unclassified Unlimited	28	**19b. TELEPHONE NUMBER** *(include area code)* (202) 767-9352

CONTENTS

I EXECUTIVE SUMMARY

In this report, we examine the formalism of coupled mode theory from several viewpoints, using the fiber optic directional coupler as a model problem to unify the discussion. With this model, we present the basic maps and tools used in describing coupled systems, emphasizing the connections between the approaches by using a consistent notation across phasor, matrix algebra, and geometrical descriptions. Novel developments include:

- a space/time phasor description of the fields in coupler propagation problems,
- a derivation of the "gauge transformation" taking coupled wave devices to the standard coupled mode formulation,
- a phasor description of the coupled state map using the conventional basis set,
- a technical discussion of the phase ambiguity in the geometric viewpoint, and a novel approach to using branch cuts and sheets from complex variable theory to resolve it,
- a careful description of the co-ordinate change to the coupled basis set,
- an analysis using similarity transforms to solve the coupled mode problem directly in the matrix description
- a description of the connection between the geometrical approach and the conventional dispersion maps in coupled wave problems.

II INTRODUCTION

Scope

This report is meant to synthesize several views of coupled mode theory, with an eye towards making connections between the geometrical approach and various analytic techniques. By viewing a standard problem, the directional coupler, we illustrate how the phasor, matrix, and geometrical views complement each other. It is not intended to be an exhaustive survey or an *ab initio* tutorial, but rather a reference for fiber-optic practitioners.

By using the directional coupler as our model problem, we show that the same formalism we have developed earlier for generalized coupled modes [1] and for propagation in birefringent networks [2, 3] can be applied directly. We make the connection between the 2×2 matrix approach which is standard for the coupler ("Jones calculus" in optics) and the 3D vector description of the same problem, weaving them together with phasor descriptions of the phase relationships. This 3D geometric description is the Poincare sphere in classical optics, and was generalized to incoherent light as the Stokes and Mueller approach [4]. The Stokes description reduces to the Poincare sphere description when one treats monochromatic light, and we restrict ourselves to this case.

Background

There are several potential pitfalls in analyzing systems with propagating waves. One is the fact that the sign convention can be counterintuitive when switching back and forth from space and time views. This is partly due to the symmetry of sine wave: since reversing the sign of the argument leaves a sine wave, the function looks the same in both z and t, which have opposite signs. Another pitfall is in tracking the phase of waves with different propagation constants: larger propagation constants mean that more phase accumulates per unit length, and thus that the wave travels more slowly. Thus, "advancing" in phase means that the wave is travelling slower. It is important to recognize that the sign of the time and space arguments changes the form of the description, so that reference formulae must be checked from different sources. We will alert the reader to these as we go.

We will discuss guided travelling waves, cast as plane waves of the form

$$g(z,t) = f(z - vt) = Ae^{j(\omega\, t\, -k\, z)}\,, \tag{1}$$

namely a sinusoidal wave travelling in the positive z direction at phase velocity $v = \omega/k$, with angular frequency ω and propagation constant $k = nk_0 = 2\pi n/\lambda_0$, where n is the phase velocity index of refraction. The zero subscripts imply the propagation constant and wavelength in vacuum.

Our model system is a directional coupler comprising a pair of waveguides that are coupled evanescently on a substrate. A standard application is that light is introduced at one of the input ports and evolves to light emerging at the two output ports with equal amplitude.

Phasor description

To help ground the discussion, we look at the *uncoupled* case: light waves of equal amplitude are introduced into two waveguides which have slightly different indices of refraction. The situation is illustrated below in Fig. 1. Light of equal amplitude and phase is introduced into input faces at each of the two waveguides (right, Fig. 1a). The mode amplitudes are sketched along the transverse dimension (axis pointing to the right and down), while the two other axes are meant to represent the field's phasor in the complex plane. The "$Re - Im$" axes define that plane, properly viewed from a vantage point up and to the left of the figure

Manuscript approved July 9, 2013.

(shown schematically as an 'eye'). The phasors, representing the optical phase $e^{j\omega t}$, rotate CCW in time, and at successively later times (snapshots progressing to the left) they have successively greater angles with respect to the real axis. This sequence represents the field at the input face with distance fixed at $z = 0$. Note that we could also view this series of time snapshots as a sequence of phasors distributed in *space*, rigidly translating as a wave towards the input face. Again, viewed properly from a vantage point up and to the left of the figures, the phasors can be viewed as varying in space as e^{-jkz}, and would now appear to be a sequence rotating in the *opposite* direction, namely CW, as z increases to the left for the observer.

Moving to the situation inside the waveguides (Fig. 1b), we assume waveguide 1 (shaded waveguide) has an index greater than that of waveguide 2. We expect the sequence of phasors to also rotate CW, e^{-jkz} as above, when we fix time and vary space by going deeper into the waveguide. In both waveguides, the phasors rotate CW, but since waveguide 1 has a greater k, its phasor rotates more rapidly as we progress to greater z. Thus, while both guides have the same phase at the input face, guide 1's phasor has gone through a greater angle at each position. Fixing attention at the output, one sees the slightly confusing situation that guide 1 has advanced more in phase. If we now let time progress, both phasors rotate at the same $e^{j\omega t}$, and the light in guide 2 will go through the real axis first. This means, for instance, that guide 2's maximum will occur at an earlier time than guide 1's maximum because it has fewer radians to move. This is the indication that the same point on a waveform (i.e. the top of a cosine cycle) happens earlier for waveguide 2: the light in waveguide 2 is travelling faster than the light in waveguide 1.

Overview

Given this basic phasor approach, we will be able to treat the phase evolutions of the system consistently. In the next two sections, we present descriptions of the coupled mode formalism in both the standard matrix algebra approach (culminating in the basic coupled mode equation, Eqn (9)) and in the geometric representation we have used earlier. A new feature of this development is an explanation of the ways in which the periodicity of the state map can be interpreted using ideas from complex variables (i.e. branch cuts and branch points). A general map is developed (Fig. 3) which exploits phasor representations. In Section V, we exercise the formalism for uncoupled waveguides, and introduce the notion that the physical character of the system is largely a matter of the viewpoint enforced by choosing a basis. Since our development does not describe coupling in the conventional sense, it illustrates the "basis prejudice" common in descriptions of physical systems. We conclude that Section by comparing the "maps" of the different basis sets, illustrating the fact that since phase is an important concept in two-state systems, one must be careful when making transformations between bases. Finally, in Section VI, we analyze the directional coupler itself. Instead of a formal mathematical development as in earlier work [1], we approach the problem from the matrix description, showing that the state evolution can be viewed as a similarity transform of the simplest uncoupled description. We conclude the Section with a discussion of the connection between directional couplers and the dispersion curves for the waveguides.

III COUPLED STATES: MATRIX FORM

Basic coupled mode equation

In our basic model, we assume a pair of waveguides evanescently coupled on a substrate. The amplitudes of the fields in the two waveguides can be cast as a 2D column vector, each entry corresponding to the amplitude of the wave in that waveguide. The formalisms for describing propagating waves that are coupled in space such as these was introduced in 1954 by Pierce [5] as a matrix representing a linear transfer function, and was applied in differential from by Yariv [6] to describe coupling in electro-optic devices in an influential

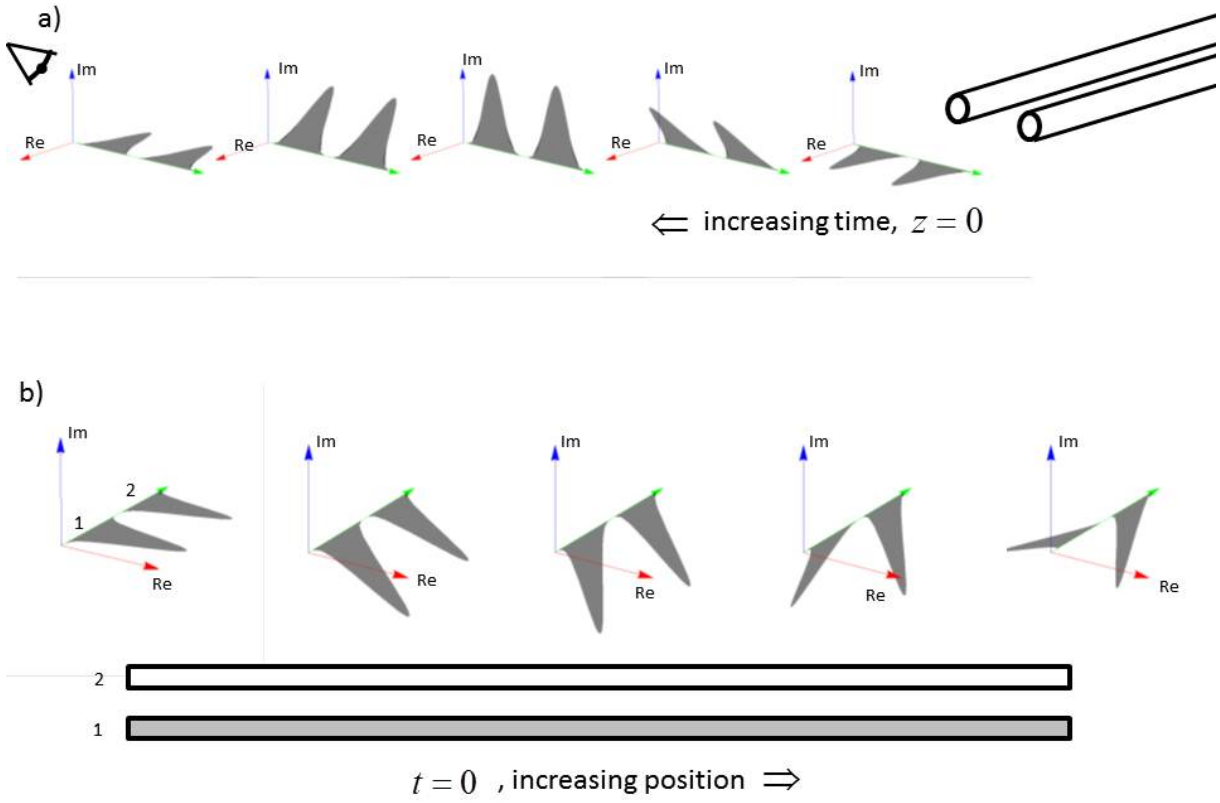

Fig. 1: Evolution in uncoupled guides (see text). (a) Phase of light at input face for a series of times (progressing to the left). Time dependence for both guides are identical ($\sim e^{j\omega t}$) and amplitudes are fixed. (b) Phases in waveguides for fixed time $t = 0$. Both phasors rotate CW in space, and mode 1 has higher index than mode 2.

article. A shortcoming of that article is its formal description of the coupling equation. A more physical description is given by Haus [7], who presents a general development with matrix elements that are tied to the system parameters. In this development, the complex amplitudes for two waves, $\bar{a}_1$ and $\bar{a}_2$, are described by a coupled differential equation with physically descriptive matrix elements. (We use barred coefficients because we will deal with a transformed version of them later.) The coupling equations can be cast in matrix form as [7]

$$\frac{d}{dz}\begin{bmatrix}\bar{a}_1\\ \bar{a}_2\end{bmatrix} = \begin{bmatrix}-jk_1 & \kappa_{12}\\ \kappa_{21} & -jk_2\end{bmatrix}\begin{bmatrix}\bar{a}_1\\ \bar{a}_2\end{bmatrix} \tag{2}$$

Physically, this equation means that

- We consider only the two modes, implicitly assuming that both describe waves propagating in the positive z direction at optical frequency ω, which is not explicitly expressed.
- In the absence of coupling (off-diagonal terms κ_{ij} are zero), each wave's amplitude, $\bar{a}_i$, advances

in phase as $\bar{a}_i(z) \sim \bar{a}_{i_0} e^{-jk_i z}$. These k_i are the wave numbers, or propagation constants, for the uncoupled modes.

- Each wave's amplitude is modified by coupling to the other wave: κ_{ij} describes the changes that amplitude $\bar{a}_i$ experiences due to the presence of amplitude $\bar{a}_j$ in the adjacent guide.
- The source of this coupling is that each wave's field creates a polarization vector, $\vec{P}$, in the other wave's waveguide, and this polarization is a driving term for the wave equation.
- If power is to be conserved[5, 6, 7], we must have $\kappa_{12} = -\kappa_{21}^*$. This makes the matrix in Eqn (2) a Hermitian matrix multiplied by $-j$, preventing the compound state from growing in amplitude.

This form is the starting point for all discussions of coupled mode systems.

Coupling constant κ

It is the presence of the off-diagonal coupling constant κ that permits the wave in one mode to influence the other. Yariv [6] details several basic forms for this, but a simplified form shown by Haus for a slab waveguide model [7] is the overlap integral between the modes,

$$\kappa_{i\,j} \;=\; \frac{-j\,\omega}{4} \int_{A_j} da(\epsilon_{in} - \epsilon)\, \hat{\mathrm{e}}_i \cdot \hat{\mathrm{e}}_j^*, \tag{3}$$

where ϵ_{in} is the dielectric constant inside the waveguide and ϵ is that for the rest of the substrate. The integration takes place over the transverse dimensions of waveguide j, namely A_j, and the transverse fields for the modes are given by the $\hat{\mathrm{e}}$. For identical waveguides, the coupling constant in Eqn (3) is seen to be purely imaginary: $\kappa_{12} = \kappa_{21} = -j\,\kappa$. Later, we will take this case as our baseline coupled system.

In general, for power-conserving systems, we can cast these coupling coefficients (looking ahead for later convenience) in terms of their real and imaginary parts as

$$\kappa_{12} \;=\; \kappa_{re} - j\kappa_{im} \;=\; -j(\kappa_{im} - j(-\kappa_{re})) \;=\; -j(\kappa_1 - j\kappa_2)$$

and

$$\kappa_{21} \;=\; -\kappa_{re} - j\kappa_{im} \;=\; -j(\kappa_{im} + j(-\kappa_{re})) \;=\; -j(\kappa_1 + j\kappa_2)$$

so that

$$\kappa_1 \equiv \kappa_{im} = -\mathit{Im}(\kappa_{12}) \qquad \kappa_2 \equiv -\kappa_{re} = -\mathit{Re}(\kappa_{12}) = \mathit{Re}(\kappa_{21}). \tag{4}$$

Note that

$$|\kappa_{12}|^2 \;=\; |\kappa_{21}|^2 \;=\; \kappa_1^2 + \kappa_2^2$$

Removing the average phase from the coupled equation

The propagation constants k_1 and k_2 are identical in the ideal coupler, but in actuality may not be identical. It useful to separate the average optical phase that both waveguides experience from the phase difference due to differing propagation constants. We decompose the propagation constants into their average and difference components, choosing k_1 as the "slow" wave (greater propagation constant) :

$$k_1 \equiv \bar{k} + \kappa_3 \quad ; \qquad k_2 \equiv \bar{k} - \kappa_3 \qquad \Longleftrightarrow \qquad \bar{k} = \frac{k_1 + k_2}{2} \quad ; \qquad \kappa_3 = \frac{k_1 - k_2}{2} \tag{5}$$

This reflects the fact that both guides have an underlying average optical propagation constant ($\bar{k}$, which might vary along the waveguide) but that the two guides may differ slightly (in this case by $2\kappa_3$). Then the coupled mode equation can be cast as

$$\begin{aligned}\frac{d}{dz}\begin{bmatrix}\bar{a}_1\\ \bar{a}_2\end{bmatrix} &= -j\begin{bmatrix}\bar{k}+\kappa_3 & \kappa_1-j\kappa_2\\ \kappa_1+j\kappa_2 & \bar{k}-\kappa_3\end{bmatrix}\begin{bmatrix}\bar{a}_1\\ \bar{a}_2\end{bmatrix}\\ &= -j\begin{bmatrix}\kappa_3 & \kappa_1-j\kappa_2\\ \kappa_1+j\kappa_2 & -\kappa_3\end{bmatrix}\begin{bmatrix}\bar{a}_1\\ \bar{a}_2\end{bmatrix} - j\bar{k}\,\mathbf{I}\begin{bmatrix}\bar{a}_1\\ \bar{a}_2\end{bmatrix}\end{aligned} \tag{6}$$

where $\mathbf{I}$ is the 2×2 identity matrix.

The overall phase due to $\bar{k}$ in Eqn (6) can be transformed away [1] by a "gauge transformation" in which the original wave amplitudes, $\bar{a}_i$, are replaced by the a_i, their "slowly varying" components:

$$\bar{a}_i(z) \;\rightarrow\; e^{-j\int \bar{k}(z)dz}\,a_i(z). \tag{7}$$

Under this transformation, the derivatives of the original wave amplitudes become

$$\frac{d\,\bar{a}_i}{dz} = -j\,\bar{k}(z)e^{-j\int \bar{k}(z)dz}\,a_i(z) + e^{-j\int \bar{k}(z)dz}\frac{d\,a_i}{dz} = -j\bar{k}(z)\bar{a}_i(z) + e^{-j\int \bar{k}(z)dz}\frac{d\,a_i}{dz}. \tag{8}$$

Substituting Eqn (8) into the left side of Eqn (6), and substituting Eqn (7) for the transformed amplitudes into the right side of Eqn (6) yields

$$\boxed{\frac{d}{dz}\begin{bmatrix}a_1\\ a_2\end{bmatrix} = -j\begin{bmatrix}\kappa_3 & \kappa_1-j\kappa_2\\ \kappa_1+j\kappa_2 & -\kappa_3\end{bmatrix}\begin{bmatrix}a_1\\ a_2\end{bmatrix}} \tag{9}$$

The implication of Eqn (9) is that the overall phase (attributed to the optical path length) can be transformed away from the differential equation. That is, one can solve Eqn (9) for the slowly varying amplitudes and then simply multiply by the overall phase, $e^{-j\bar{\phi}} = e^{-j\int \bar{k}(z)dz}$, at the end of the problem to regain the original "correct" barred amplitudes[1]. This separability of the overall phase has been exploited in the geometrical representation for problems that require total phases[2, 3], such as interferometers.

Eqn (9) is the basic equation of coupled mode theory for power conserving systems in which the overall phase is suppressed. Recall that for identical coupled waveguides, Eqn (4) implies that only $\kappa_1 \neq 0$.

IV COUPLED STATES: GEOMETRIC FORM

Normal form

The wave amplitudes a_1 and a_2 are the complex wave amplitudes for the two guides, which we can consider as the components of the total state of the coupler, $|\psi_{tot}\rangle$. This state represents everything we know about the system. But we are applying two constraints by (1) ignoring the overall phase, and (2) requiring power conservation. Thus, a "reduced" state of the system can be described with two degrees of freedom (DOF), and these can be represented by the latitude and longitude of a point on a unit sphere. In particular, we can simplify the total state to this reduced state as

$$|\psi_{tot}\rangle \sim \{\rho e^{-j\bar{\phi}}\}\begin{bmatrix}\cos(\theta/2)e^{-j\phi/2}\\ \sin(\theta/2)e^{+j\phi/2}\end{bmatrix} \Longrightarrow\; |\psi\rangle \sim \begin{bmatrix}\cos(\theta/2)e^{-j\phi/2}\\ \sin(\theta/2)e^{+j\phi/2}\end{bmatrix} \tag{10}$$

[1]There is no mathematical adiabatic restriction to "slowly varying" functions, but the unidirectional Eqn (9) requires no reflected waves.

We call Eqn (10) the "normal form" and it has several implicit assumptions and conventions:

- We introduce the description of our system as an abstract vector, $|\psi\rangle$. This vector exists independently of the basis set in which it is described.
- The "$\sim$" symbol is used to distinguish between the abstract state vector and the two dimensional column which represents the co-ordinates of the state vector in the assumed basis set. In other words, "the map is not the territory:" a vector is not a set of coordinates. At the moment, we are describing it in the bases corresponding to unit amplitudes in the two waveguides.
- The terms in braces are the two DOF that we have suppressed, namely an overall magnitude for the vector, ρ (assumed unity for power conservation), and the overall phase $\bar{\phi} = \int \bar{k}(z)dz$ (which is ignored, since it can be reclaimed at the end). The seemingly redundant factors of 2 are to make the geometric representation more easily used.
- The angle θ is the polar angle in the geometrical map. Its range is $0 \leq \theta \leq \pi$. Thus, $\theta = 0$ corresponds to unit magnitude in waveguide 1, the top co-ordinate, with zero magnitude in the other waveguide, while $\theta = \pi$ is the reverse.
- This convention means that the "north pole" ($\theta = 0$) and the "south pole" ($\theta = \pi$) correspond to the two basis vectors for the states (namely, unit amplitude in each of the waveguides), and thus that the polar angle is a measure of the relative amplitudes of the waves in those waveguides.
- The angle ϕ is the phase angle between the two waveguide amplitudes, its range is $-\pi \leq \phi \leq +\pi$ to map onto the azimuthal angle in the geometrical map. That is, the azimuthal angle of the state's vector is the phase difference (modulo 2π) between the waveguide components.
- Once the magnitude and the overall phase are stripped away, the arrow indicates that only the two angles, θ and ϕ, are needed to represent the relative amplitudes and phases of the components, the two DOF we consider.
- We have used the "positive frequency" convention for time, and thus a wave propagating towards more positive z coordinates will change phase as $\sim e^{-jkz}$. This takes a bit of getting used to. One way of viewing it is to visualize a phasor representation as in the Introduction: as time progresses, the phasor representing the wave will rotate CCW in the "positive" direction. To follow a given point on the waveform, one would have to advance in z to keep up with the wave, "unwinding" the phase accrued over time by rotating in the "negative" direction (CW) as one proceeds down the z axis.

Mapping normal form to 3D representation

The utility of the geometric representation is that it leads to a coordinate-free description: a state is then represented by a point on the sphere, and we can often describe its trajectory by using geometrical means, such as an equation of motion (described later). Thus, we want to be able to switch back and forth between the 2D normal form vector and the 3D representation with ease. To do this, we need a "map" as described below. We assume an orthogonal basis set for the 3D representation, namely $\{\hat{\mathbf{e}}_1, \hat{\mathbf{e}}_2, \hat{\mathbf{e}}_3\}$.

We associate two basis state vectors, which correspond to the standard basis vectors in 2D,

$$|1\rangle \sim \begin{bmatrix} 1 \\ 0 \end{bmatrix} \quad ; \quad |2\rangle \sim \begin{bmatrix} 0 \\ 1 \end{bmatrix},$$

and represent them in the geometrical representation as the north and south poles of a unit sphere, namely unit vectors $\pm\hat{\mathbf{e}}_3$. Then any state expressed in the normal form has a unique latitude and longitude, i.e. a unique θ and ϕ, and thus a unique position on the surface of the unit sphere, as shown below.

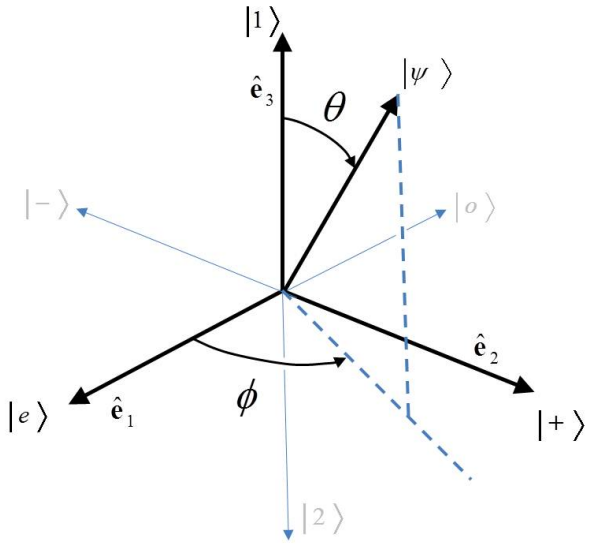

Fig. 2: Geometric representation of states. The 'top' state, $|1\rangle$ is at the north pole ($\theta = 0$), corresponding to unit amplitude in waveguide 1. General state $|\psi\rangle$ is represented by polar angle θ and azimuthal angle ϕ, which represent relative amplitudes and phases between fields in the waveguides, respectively.

A general state is shown in Fig. 2, which highlights three of the principal states often used in describing the system behavior. The "north pole," or $\hat{\mathbf{e}}_3$ is state $|1\rangle$, the "top" basis vector (i.e. the field is only in waveguide 1). In light of the normal form, Eqn (10), it must be that $\theta = 0$, and, since no light is in the other state, the phase ϕ is indeterminate. The state given by $|e\rangle = \frac{1}{\sqrt{2}}\begin{bmatrix} 1 \\ 1 \end{bmatrix}$ is called the "even" state since it is the symmetric (equal amplitude, zero phase difference) superposition of the two basis states. Thus, in the 3D representation, it defines the axis for which the azimuthal angle is zero. It corresponds to $(\theta = \pi/2,\ \phi = 0)$, which is defined as $\hat{\mathbf{e}}_1$. The third labelled state, $|+\rangle$, is the "phase advanced" state. Since $\theta = \phi = \pi/2$ for this state, it corresponds to $\hat{\mathbf{e}}_2$ in the 3D representation, and in the standard basis it is represented in normal form as $\frac{1}{\sqrt{2}}\begin{bmatrix} e^{-j(\pi/2)/2} \\ e^{+j(\pi/2)/2} \end{bmatrix}$: the phase of the component in state $|1\rangle$ is $\pi/4$ more advanced than the average phase, while the component in orthogonal state $|2\rangle$ is $\pi/4$ behind the average phase. Thus the top component (guide 1) is advanced by $\pi/2$ with respect to the bottom component (guide 2). From the viewpoint of $|1\rangle$, state $|+\rangle$ has been rotated in a positive sense (right hand rule) from $|e\rangle$, the zero-phase state, while from the viewpoint of state $|2\rangle$, state $|+\rangle$ has been rotated in a negative sense from $|e\rangle$. Physically, this means that for state $|+\rangle$, its component from $|1\rangle$ has acquired more phase ($e^{-j\pi/4}$), while its component from $|2\rangle$ has lost phase, ($e^{+j\pi/4}$). That is, the component in $|1\rangle$ is the "slower" of the two components: it has a larger propagation constant, and acquire more phase every meter than does the component in $|2\rangle$.

Note that in the geometric representation, both $|e\rangle$ and $|+\rangle$ are at an angle of $\pi/2$ from the basis vector $|1\rangle$, but their amplitudes (see Eqn (10)) in that basis state are the cosine of half that angle, namely $cos\,\frac{\pi}{4} = \frac{1}{\sqrt{2}}$. This illustrates the general point that angles in the geometrical representation are twice the "real" angles: two states that are orthogonal must be on opposite sides of the sphere. Thus the states orthogonal

to $|1\rangle$, $|e\rangle$, and $|+\rangle$, are $|2\rangle$, $|o\rangle$, and $|-\rangle$, (bottom basis, odd (or anti-symmetric), and phase retarded states, respectively) and are located on the corresponding opposite sides of the sphere.

In light of the above, we see that the state shown in Fig. 2 has most of its power in waveguide 1, and the phase of the light in waveguide 1 is phase advanced with respect to the light in waveguide 2 by ϕ. An important point to note from Eqn (10) is the "cosine half-angle projection" property, i.e. that the amplitude of a unit state, projected onto another, is given by the cosine of half the angle between their vectors. That is, for instance, the amplitude of $|\psi\rangle$ in Fig. 2, projected onto state $|1\rangle$ is $cos\,\frac{\theta}{2}$, from the normal form, while its amplitude projected onto state $|2\rangle$ is $cos\,\frac{\pi-\theta}{2} = sin\,\frac{\theta}{2}$: the left side of this relation is from the geometrical construction (since the angle from $|\psi\rangle$ to $|2\rangle$ is $\pi - \theta$), while the right side is from the normal form, Eqn (10).

The above property, the cosine half-angle projection, is true between any two states generally: by suitable co-ordinate transformation, one can always move one of the states to $|1\rangle$ and then project onto it as in Eqn (10). This leads to a real advantage for the geometrical representation: it permits a direct visualization of changes in basis states. Consider the field shown in Fig. 2 as state $|\psi\rangle$. In the basis we have chosen, it represents the labelled distinct values of relative amplitudes for the two guides, and relative phases between the fields. If we were to change the basis, for instance, so that the even and odd superposition states $|e\rangle$ and $|o\rangle$ were used as basis states, the actual *fields* in the guides would be the same, and they would correspond to that same point on the unit sphere (and thus the same state $|\psi\rangle$) but the *coordinates* of that point, its latitude and longitude with respect to $|e\rangle$ and $|o\rangle$, would be different. Properly viewed, this is a liberating viewpoint to adopt: any two antipodal points can become a basis set, and we are free to choose them as a basis to suit our convenience. Thus, a given trajectory for a state can be analyzed instantly in terms of other physical bases. In the next few sections, we will illustrate several views of the basic coupler model.

State map: technical details

To flesh out this map, the phasor characteristics of the states are shown in Fig. 3, below, using the same hybrid phasor notation we used in Fig. 1. For instance, state $|e\rangle$ is seen to be the even combination of the two basis states, $|1\rangle$ and $|2\rangle$, while state $|+\rangle$ is the state for which the phase difference between the bases is $\pi/2$ (i.e. the bases are advanced and retarded by $\pi/4$, respectively, as in the normal form, Eqn (10)).

While the phase difference between components in the two bases can grow without bound, the map can only display one transit of the sphere, 2π radians. This leads to a technical issue which we address here. Consider how states with increasing phase difference in Eqn (10) would be represented: we imagine starting with state $|e\rangle$, changing only the relative phase between the components, and observing how the states are mapped. State $|e\rangle$ has zero phase difference and as one increases the phase difference, the state would evolve along the equator, reaching state $|+\rangle$ when the phase difference reaches $\pi/2$ (i.e. $\pm\pi/4$), and finally arriving at the state labelled $|o_+\rangle$ as the phase approaches π (Fig. 3). On the other hand, if we started at state $|e\rangle$ and *decreased* the phase difference, the state would first evolve to $|-\rangle$ and then approach the state labelled $|o_-\rangle$ as the phase difference approaches $-\pi$. It seems as if state $|o\rangle$ has two different representations: $|o_+\rangle$ and $|o_-\rangle$ have distinctly different shapes in Fig. 3, depending on the path taken from state $|e\rangle$.

What is going on is that the sphere is a "cover" for the phases: it can only represent phases modulo 2π. This is shown in Fig. 4. Technically, we can view the sphere as a "sheet" covering phases $-\pi \leq \phi \leq \pi$, and as the phase increases past state $|o_+\rangle$ (i.e. on its way from $|e\rangle$ through $|+\rangle$ to $|o_+\rangle$ and then beyond $|o_+\rangle$), it passes over a "branch cut" at $\phi = \pi$ onto *another* sheet, this one representing $\pi \leq \phi \leq 3\pi$. Points on this sheet (for increasing ϕ) have 2π more phase than equivalent points on the first sheet. On *this* sheet, the state whose phase has recently become greater than π now has a phase co-ordinate $\approx -\pi$ but has an additional phase of 2π by virtue of having passed onto this new sheet. Thus, in going from $|e\rangle$ to $|o_+\rangle$, the phase difference has increased by π (shown as $\pm\pi/2$ in Fig. 3). Just as it passes over $|o\rangle$, the co-ordinate

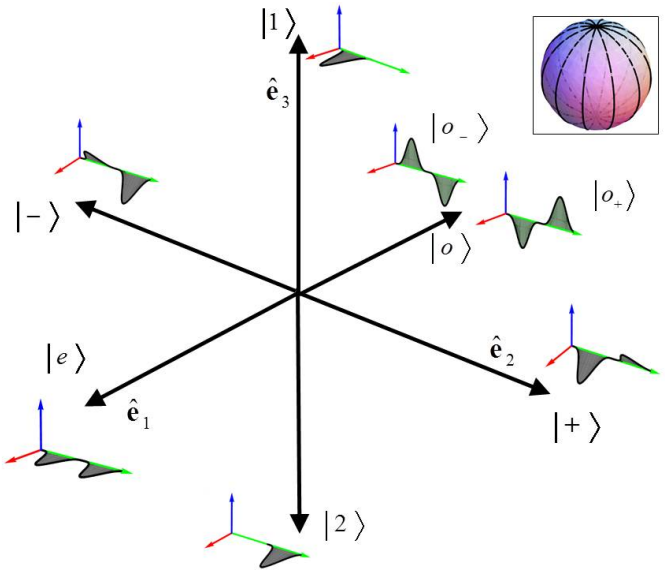

Fig. 3: Map of states as phasors using normal basis. Note apparent discontinuity associated with state $|o\rangle$. Inset: longitude lines of equal phase difference.

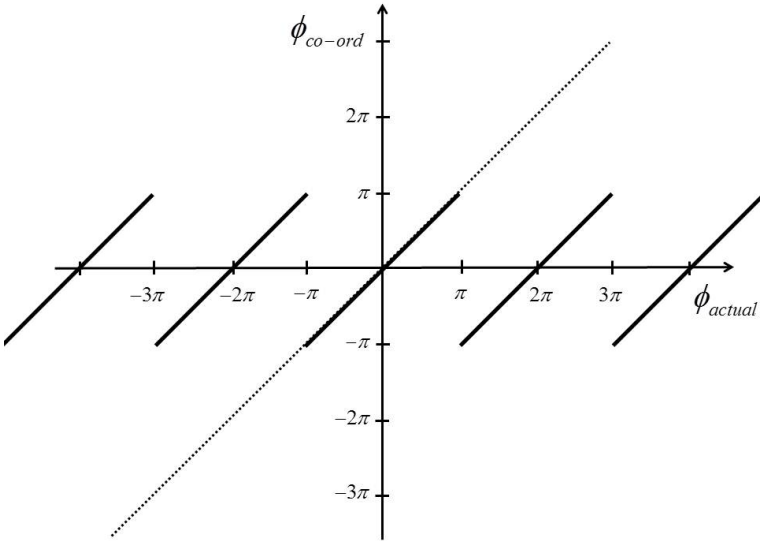

Fig. 4: Phase co-ordinate plotted vs. actual phase. Since the co-ordinate for the state is limited to $-\pi \leq \phi \leq \pi$, phases must be 'reset' every 2π radians. The actual phase is continuous (dotted line) but its co-ordinate representation is not (heavy line segments).

changes from $+\pi$ to $-\pi$ while the phase has simultaneously jumped by 2π from passing onto the new sheet. Thus, the phase is continuous, while the co-ordinates change discontinuously across the branch cut. This sheet is illustrated in Fig. 5 as being outside the original sheet for increasing ϕ. In a similar way, if we view states with decreasing phase, the state passes onto another sheet (shown as inside the original sheet in Fig.

5) as it crosses the branch cut, but this sheet is displaced by -2π.

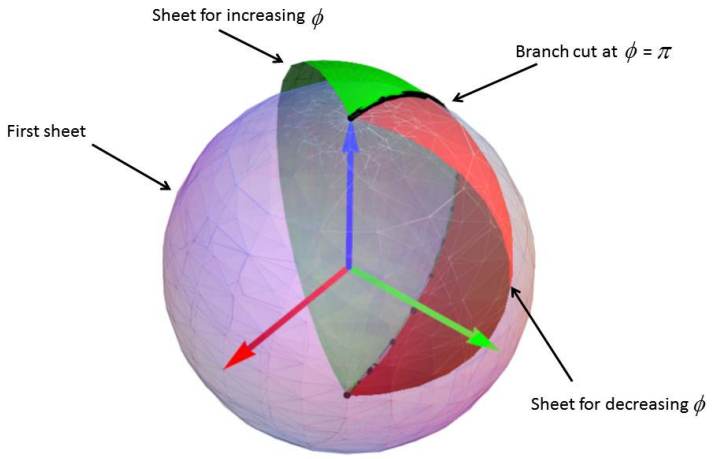

Fig. 5: Sketch of sheets folded at branch cut. As phase increases past $\phi = \pi$, the state moves to another sheet (green sheet, partially shown, outside first sheet) as it passes over branch cut. Conversely, for phases decreasing below $-\pi$, the state moves to a different sheet (red sheet, partially shown, inside first sheet) as it passes over the branch cut. Each set of co-ordinates implicitly describes points on other sheets.

What is clear from this rather technical discussion is that this is a "co-ordinate problem" not a "state problem:" nothing discontinuous happens to the state, the apparent discontinuity is an artifact of the map's cyclical re-use of a fixed range of longitude co-ordinates. This is somewhat analogous to the situation in solid state physics in which the wavevector of an accelerating Bloch electron is "umklapped" back to the other side of the Brillouin zone to keep its wavevector in the first Brillouin zone. In our case, the phase difference is increasing monotonically (we imagine a counter that keeps track of the times the state has wound around the branch cut) but the representation looks non-monotonic.

The branch points at which the branch cut ($\phi = \pi$) ends are the two basis states, $|1\rangle$ and $|2\rangle$. One can visualize the sheets being "folded in" at these singular points, as shown in Fig. 5. The singularity at the branch points can be seen in light of the normal form, Eqn (10), and Figs. 3 and 5. That is, all states on lines of a given longitude have the same phase difference between their components, regardless of their relative amplitudes (i.e. latitude). At the poles, however, only one component exists, so the phase difference is meaningless. Thus, if we imagine traversing a small circle near the north pole, the phases on that circle go through a range of 2π, but as the circle (with a continuum of longitudes) shrinks to the point of the pole, there is only one state. Again, the states are continuous but the co-ordinates are discontinuous.

As a practical matter, the discontinuities due to the branches and branch points are inconsequential. The issue is really only a co-ordinate problem, not a mapping problem, and any trajectory of a state will evolve smoothly and continuously: in terms of the co-ordinate mapping to a "covering" range of 2π, however, it may look discontinuous.

V STATE EVOLUTION IN UNCOUPLED GUIDES

The simplest case of the general coupled mode equation is for two uncoupled waveguides: since there is no coupling between them, their fields propagate independently.

Identical waveguides

When two uncoupled waveguides are identical, their propagation constants are identical, and by virtue of Eqn (5), we have $k_1 = k_2 = \bar{k}$ and $\kappa_3 = 0$. Since there is no coupling, $\kappa_1 = \kappa_2 = 0$ by virtue of Eqn (4). From the basic coupled mode equation we then have

$$\frac{d}{dz}\begin{bmatrix} a_1 \\ a_2 \end{bmatrix} = -j\begin{bmatrix} 0 & 0 \\ 0 & 0 \end{bmatrix}\begin{bmatrix} a_1 \\ a_2 \end{bmatrix} \Longrightarrow \begin{bmatrix} a_1 \\ a_2 \end{bmatrix} \; constant.$$

If the 2D state vector remains constant, then the normal form implies that the 3D representation also remains constant, so the state vector shown in Fig. 2 remains fixed. This is as expected: since the amplitudes in each waveguide remain unchanged, θ remains unchanged; since the waves suffer identical phase shifts as z progresses, there is no change in their phase difference and ϕ remains constant. What has been omitted, of course, is that in propagating down the waveguides there is a continual advance of phase, which we would expect to describe with the slowly-varying gauge transformation, Eqn (7).

Distinct waveguides – normal basis

A more interesting case is for uncoupled waveguides with different propagation constants. Then $\kappa_1 = \kappa_2 = 0$, since they are uncoupled, but $k_1 \neq k_2$ implies that $\kappa_3 \neq 0$. In this case, Eqn (9), the coupling equation, becomes

$$\frac{d}{dz}\begin{bmatrix} a_1 \\ a_2 \end{bmatrix} = -j\begin{bmatrix} +\kappa_3 & 0 \\ 0 & -\kappa_3 \end{bmatrix}\begin{bmatrix} a_1 \\ a_2 \end{bmatrix} = -j\begin{bmatrix} +\kappa_3\, a_1 \\ -\kappa_3\, a_2 \end{bmatrix}. \tag{11}$$

The solution is immediate: $a_{1,2} \sim e^{\mp j\kappa_3 z}$ with the implication that the phase of wave 1 (assumed to be the "slow" mode) advances with respect to that of waveguide 2. Indeed,

$$\begin{bmatrix} a_1(z) \\ a_2(z) \end{bmatrix} = \begin{bmatrix} e^{-j\kappa_3 z} & 0 \\ 0 & e^{+j\kappa_3 z} \end{bmatrix}\begin{bmatrix} a_1(0) \\ a_2(0) \end{bmatrix} = \begin{bmatrix} a_1(0)e^{-j\kappa_3 z} \\ a_2(0)e^{+j\kappa_3 z} \end{bmatrix} = \begin{bmatrix} (cos\frac{\theta_i}{2}e^{-j\phi_i/2})e^{-j\frac{2\kappa_3 z}{2}} \\ sin\frac{\theta_i}{2}e^{+j\phi_i/2})e^{+j\frac{2\kappa_3 z}{2}} \end{bmatrix} \tag{12}$$

Cast in this form, Eqn (12) permits direct comparison to Eqn (10): θ is fixed at its initial value, θ_i, since the amplitudes remain constant, while ϕ increases linearly with distance, namely $\Delta\phi = 2\kappa_3 z$. That is, the slow guide is monotonically accumulating phase with respect to the fast guide at a rate which is the difference between the propagation constants (Eqn (5)). Note that in this case, too, angles in the geometric representation seem doubled compared to the matrix representation since it is cast in terms of difference between the mean and the phases of the two waveguides. The motion of the state vector as the waves progress down the two guides is then a precession about the $\hat{\mathbf{e}}_3$ axis, as shown in Fig. 6.

This situation is described as "uncoupled, asynchronous" propagation: the two waveguide modes do not exchange power (uncoupled, since θ is constant) but there is a continual phase slippage between them (ϕ increases monotonically): their phases are asynchronous.

Distinct waveguides – alternate basis

As mentioned above, the geometric view permits easy visualizations for a change of basis. In particular, we show here a change of basis to the even and odd states, a basis that will later be seen as important.

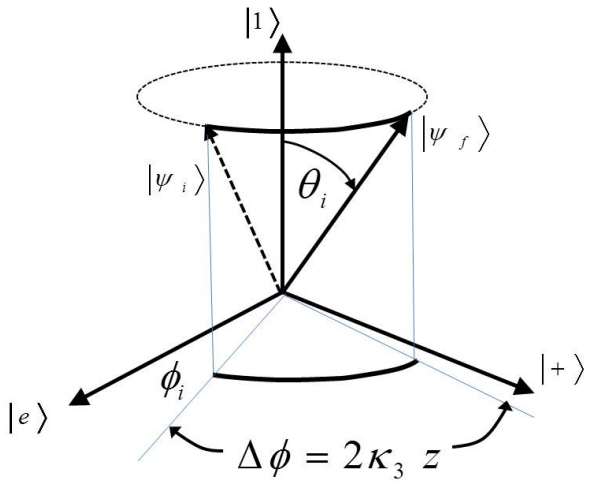

Fig. 6: Uncoupled, asynchronous evolution. The relative amplitudes remain the same (θ is constant), but the relative phase difference increases monotonically.

Alternate basis

Now consider the system viewed in a different basis, which we will denote by stars as $|1^*\rangle$ and $|2^*\rangle$. We will take these new basis vectors to be the states $|e\rangle$ and $|o\rangle$, respectively. While we could re-draw the map with these states as the north and south poles, the *most* useful view is generally to view the states as primary and re-draw the co-ordinate axes. Thus the *new* primary axis runs between $|1^*\rangle$ and $|2^*\rangle$, and the new co-ordinates are referred to this axis. From the definitions of the cardinal points in normal form, we can express each of them as superpositions of their new basis states, and hence in terms of the original basis states. We find that

$$|1^*\rangle \equiv |e\rangle \qquad\qquad |2^*\rangle \equiv |o\rangle$$

$$|e^*\rangle = \frac{1}{\sqrt{2}}(|1^*\rangle + |2^*\rangle) = \frac{1}{\sqrt{2}}(|e\rangle + |o\rangle) = |+\rangle$$

$$|+^*\rangle = \frac{1}{\sqrt{2}}(e^{-j\pi/4}\,|1^*\rangle + e^{+j\pi/4}\,|2^*\rangle) = e^{-j\pi/4}\,|1\rangle$$

$$|o^*\rangle = \frac{1}{\sqrt{2}}(e^{-j\pi/2}\,|1^*\rangle + e^{+j\pi/2}\,|2^*\rangle) = e^{-j\pi/2}\,|-\rangle$$

$$|-^*\rangle = \frac{1}{\sqrt{2}}(e^{+j\pi/4}\,|1^*\rangle + e^{-j\pi/4}\,|2^*\rangle) = e^{+j\pi/4}\,|1\rangle\,. \tag{13}$$

These relationships are plotted in Fig. 7 below. Thus, for instance, $|e^*\rangle$ in the second line above is defined in the left equality by appealing to the normal form, the basis definitions are used in the second equality, then the geometric sums are constructed and compared to Fig 3 for the last equality. As the inset shows, the lines of constant phase difference are now oriented differently than for the normal basis. Indeed, viewing the phase of the $|1^*\rangle$ component (the leftmost component in the graphical sums in Fig. 7), one sees that in

going from state $|-^*\rangle \rightarrow |e^*\rangle \rightarrow |+^*\rangle \rightarrow |o^*\rangle$, the phase of the $|1^*\rangle$ component changes monotonically as it rotates CW in the $Re - Im$ frame. The figure shows the superposition of the two basis states and

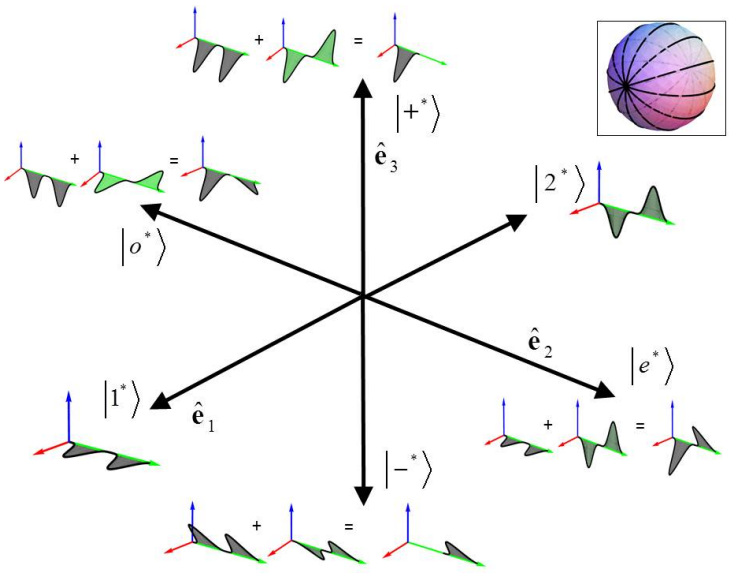

Fig. 7: Map of states as phasors using even-odd basis. Inset: lines of constant phase difference between basis states.

their resultant sums. When the Figs 3 and 7 are placed side-by-side, one sees that there are additional phases involved. That is, for instance, the state $|-^*\rangle$ is not exactly the same as state $|2\rangle$, but has an extra phase shift of $\pi/4$. This is a manifestation of the fact that the phase differences seen in the insets have fundamentally different orientations. Such extraneous phase relationships often occur in polarization optics when transforming from one basis to another, and are related to the unitary transformations that create the co-ordinate transformations: they are ultimately rotations and rotations do not commute.

Uncoupled waveguides in alternate basis

Returning to the "uncoupled, asynchronous" state evolution described in Fig. 6, we now address the evolution of the system in our new basis set. That is, we want the same trajectory of states in Fig. 6 to be described in our new co-ordinate system. In the new system, the co-ordinates are constructed by projecting states onto the $|1^*\rangle$ and $|2^*\rangle$ basis set, finding the angles, and using the normal form, Eqn (10). The projection onto $|1^*\rangle$ is given by half the angle of θ_e, the angle to $|1^*\rangle$. Our discussion above shows that the azimuth in this basis is measured from $|e^*\rangle$, which provides ϕ_e for the normal form. In this basis, note that *now* the modes are viewed as "coupled" since there is power exchanged between them. That is, angle θ_e varies as the state cycles around in Fig. 9, and thus the amplitudes in the two modes vary by virtue of Eqn. (10). The relative phase, however, is bounded as the state follows its trajectory. (There is more to it, but it requires introducing "fiducial paddles" [2, 3].) Thus, in this basis, the system is said to be displaying "coupled, synchronous" behavior. In other words, what looks like uncoupled "beating" of independent modes in one basis set, can be viewed as a synchronous power transfer between modes in another basis set.

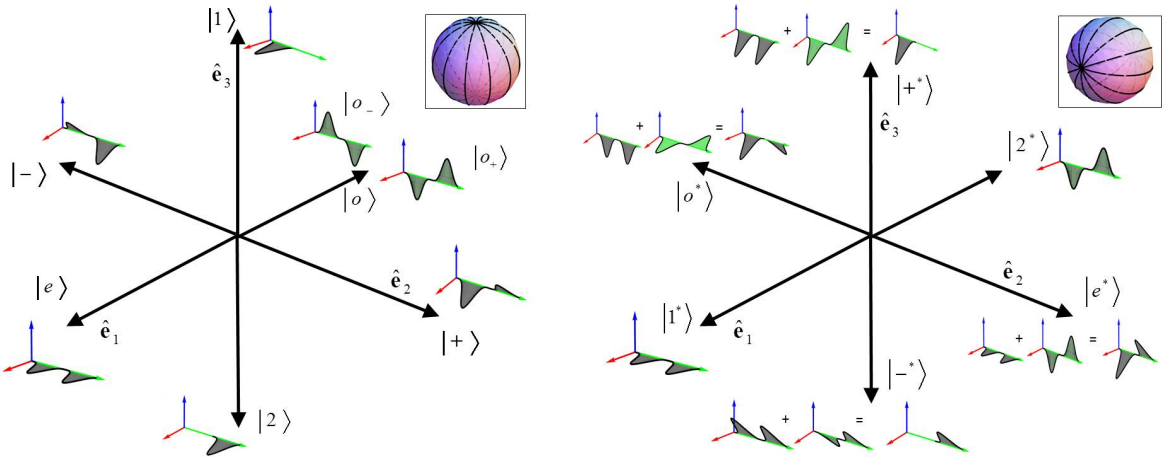

Fig. 8: Comparison of states for two basis sets.

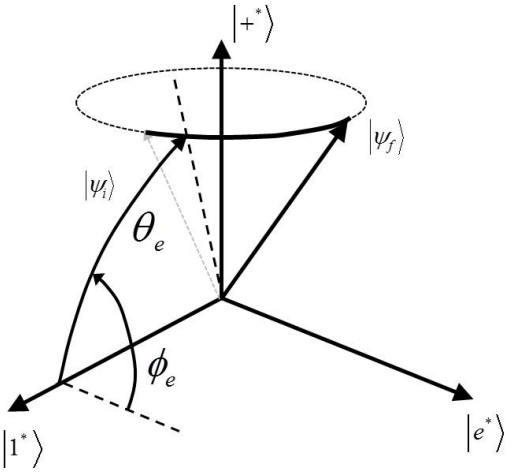

Fig. 9: "Uncoupled, asynchronous" evolution in Fig. 6, as viewed in another basis. In this basis, power varies as the state evolves.

VI STATE EVOLUTION IN COUPLED GUIDES: THE DIRECTIONAL COUPLER

Form of vector evolution

The simple case above encapsulates a great deal of the coupled mode formalism. The key point is that the coupled mode formalism is generally described by a rotation of the state vector about some axis: that axis, and the angular velocity of the rotation about it, are determined by the matrix in the basic equation, Eqn (9). Regardless of basis, the state evolves on some trajectory, and the overall state can viewed in different bases with different physical pictures. That is, the same underlying phenomena can be viewed in different ways, depending on the basis employed, and we are free to choose any basis which is convenient. This makes the study of such systems, whether coupled waveguides, polarization optics, or atomic systems, much richer

and more susceptible to physical insight and intuition [8].

What makes such physical systems yield to detailed geometrical analysis is the ability to express the behavior in the language of linear algebra and vectors, to which we now turn. This development is familiar from classical optics as the Jones calculus, Poincare sphere, Stokes, and Mueller calculus [4, 9]. The connection between the matrix view (the "Jones" view in polarization optics) and the geometric view (the "Stokes/ Poincare" view in polarization optics) is founded in the representation theory of matrices. The 2×2 complex matrices are spanned by the identity matrix and the three Pauli matrices

$$\sigma_0 = \begin{bmatrix} 1 & 0 \\ 0 & 1 \end{bmatrix}; \quad \sigma_1 = \begin{bmatrix} 0 & 1 \\ 1 & 0 \end{bmatrix}; \quad \sigma_2 = \begin{bmatrix} 0 & -j \\ +j & 0 \end{bmatrix}; \quad \sigma_3 = \begin{bmatrix} 1 & 0 \\ 0 & -1 \end{bmatrix}. \tag{14}$$

Thus, any matrix $\mathbf{K}$ can be expressed as $\mathbf{K} = \kappa_i \sigma_i$ for four complex numbers κ_i (implied summation). If $\mathbf{K}$ is Hermitian and traceless, then the κ_i are three real numbers for $i = 1, 2, 3$, which can be viewed as a vector triplet $(\kappa_1, \kappa_2, \kappa_3) \equiv \vec{\kappa}$. Viewing Eqn (11), one sees that it is of form

$$\frac{d}{dz}\begin{bmatrix} a_1 \\ a_2 \end{bmatrix} = -j\begin{bmatrix} +\kappa_3 & 0 \\ 0 & -\kappa_3 \end{bmatrix}\begin{bmatrix} a_1 \\ a_2 \end{bmatrix} = -j\kappa_3\begin{bmatrix} +1 & 0 \\ 0 & -1 \end{bmatrix}\begin{bmatrix} a_1 \\ a_2 \end{bmatrix} = -j\kappa_3\sigma_3\begin{bmatrix} a_1 \\ a_2 \end{bmatrix}. \tag{15}$$

In this case, the coupling matrix is characterized by only the third component, so we can associate the vector $\vec{\kappa} = \kappa_3\hat{\mathbf{e}}_3$. Notice that the vector for $|\psi\rangle$ then rotates about $\vec{\kappa}$ at a rate of $2\kappa_3$, by virtue of Eqn (12). As we will show below, this result is completely general as long as K is Hermitian and traceless. For such conservative systems, the coupled mode equation (Eqn (9)) can be expressed as

$$\frac{d}{dz}\begin{bmatrix} a_1 \\ a_2 \end{bmatrix} = -j\begin{bmatrix} \kappa_3 & \kappa_1 - j\kappa_2 \\ \kappa_1 + j\kappa_2 & -\kappa_3 \end{bmatrix}\begin{bmatrix} a_1 \\ a_2 \end{bmatrix} = -j(\kappa_i\sigma_i)\begin{bmatrix} a_1 \\ a_2 \end{bmatrix} = -j\vec{\kappa}\cdot\vec{\sigma}\begin{bmatrix} a_1 \\ a_2 \end{bmatrix}, \tag{16}$$

and when it is, it means that the geometric representation for state $\begin{bmatrix} a_1 \\ a_2 \end{bmatrix}$ will rotate about the vector $\vec{\kappa}$ at a rate of $2\,|\vec{\kappa}|$. Thus, Eqn (16) shows that the vector $\vec{\kappa}$ is the geometrical representation of the matrix operator in Eqn (9).

Matrix analysis

Differential equation for state

Eqn (16) is the general form that the coupling can take: κ_3 accounts for "detuning," or mismatches in the waveguide propagation constants, while κ_1 and κ_2 describe the coupling between the waveguides. Direct solutions of Eqn (16) have been tabulated [10] for conservative systems such as these. Here, we approach the problem in a way that highlights the application to a geometrical representation. Setting

$$\bar{\kappa} = |\vec{\kappa}| = |\kappa_1\hat{\mathbf{e}}_1 + \kappa_2\hat{\mathbf{e}}_2 + \kappa_3\hat{\mathbf{e}}_3| = \sqrt{\kappa_1^2 + \kappa_3^2 + \kappa_3^2},$$

there must be (see Fig. 10) angles θ_0 and ϕ_0 such that magnitude $\bar{\kappa}$ can be factored out of the coupling equation, Eqn (16):

$$\frac{d}{dz}\begin{bmatrix} a_1 \\ a_2 \end{bmatrix} = -j\begin{bmatrix} \kappa_3 & \kappa_1 - j\kappa_2 \\ \kappa_1 + j\kappa_2 & -\kappa_3 \end{bmatrix}\begin{bmatrix} a_1 \\ a_2 \end{bmatrix}$$

$$\frac{d}{dz}\begin{bmatrix} a_1 \\ a_2 \end{bmatrix} = -j\bar{\kappa}\begin{bmatrix} \cos\theta_0 & \sin\theta_0\, e^{-j\phi_0} \\ \sin\theta_0\, e^{+j\phi_0} & -\cos\theta_0 \end{bmatrix}\begin{bmatrix} a_1 \\ a_2 \end{bmatrix} = -j\bar{\kappa}D\begin{bmatrix} a_1 \\ a_2 \end{bmatrix} \tag{17}$$

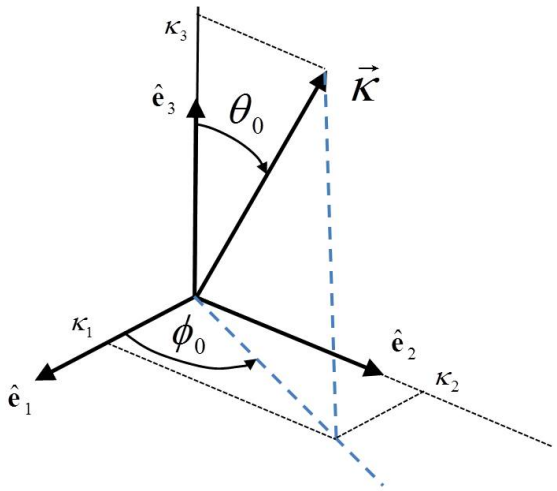

Fig. 10: Vector $\vec{\kappa}$ represents three components (κ_i) in the coupling matrix. This vector can be chararacterized by its length $|\vec{\kappa}|$ and two angles, θ_0 and ϕ_0.

The matrix D, defined in this equation, is the generator for this system:

$$D = \begin{bmatrix} \cos\,\theta_0 & \sin\theta_0\, e^{-j\phi_0} \\ \sin\theta_0\, e^{+j\phi_0} & -\cos\,\theta_0 \end{bmatrix} \tag{18}$$

Eigenbasis and similarity transforms

The eigenvectors for D are given by

$$|s\rangle \;\sim\; \vec{s} \sim \begin{bmatrix} \cos\,\frac{\theta_0}{2}\, e^{-j\phi_0/2} \\ \sin\,\frac{\theta_0}{2}\, e^{+j\phi_0/2} \end{bmatrix} \qquad |f\rangle \;\sim\; \vec{f} \sim \begin{bmatrix} \sin\,\frac{\theta_0}{2}\, e^{-j\phi_0/2} \\ -\cos\,\frac{\theta_0}{2}\, e^{+j\phi_0/2} \end{bmatrix} \tag{19}$$

where we have labelled the states to conform to our earlier descriptions as "slow" and "fast" [2, 3], and where the eigenvalues are ± 1. Clearly, $\vec{s}$ is in the normal form for a vector such as in Fig. 2. In fact, $\vec{s}$ is *explicitly* $\hat{\kappa}$, the unit vector along the direction of $\vec{\kappa}$. We will see that the differential equation for the state evolution will be a rotation about this unit vector, as noted above.

It can be shown [2] that $\vec{f}$ can also be cast as a state in normal form with $\theta_0 \rightarrow \pi - \theta_0$ and $\phi_0 \rightarrow \phi_0 - \pi$ and multiplied by a constant phase factor $e^{-j\pi/2}$. This is the state on the opposite side of $\vec{s}$ in the geometrical representation [2] and the phase factor indicates that the "fiducial paddle" for this state [2, 3] is rotated by π radians.

Creating a matrix from the adjoints of $\vec{s}$ and $\vec{f}$, we can create a matrix $S^\dagger$ that transforms co-ordinates in our conventional basis to the basis defined by eigenstates $\vec{s}$ and $\vec{f}$, and a matrix S that does the reverse. That is, we can view matrix $S^\dagger$ as being formed with the top row set as $\langle s| \;\sim\; \vec{s}^\dagger$ and bottom row set as $\langle f| \;\sim\; \vec{f}^\dagger$. When this matrix operates on any 2D vector, it dots that vector into $\langle s|$ and enters this as the top component of the new vector and similarly for $\langle f|$ as the bottom component. That is, it transforms the co-ordinates of the vector in the original basis to the co-ordinates of the same vector in the $\vec{s} - \vec{f}$ basis, i.e. it takes $|s\rangle \Longrightarrow |1\rangle$. In a similar way, the matrix S comprises the column vectors $\vec{s}$ and $\vec{f}$ and creates the inverse operation, taking $|1\rangle \Longrightarrow |s\rangle$. Using our normal forms,

$$S^\dagger = \begin{bmatrix} \cos\frac{\theta_0}{2}\, e^{+j\phi_0/2} & \sin\frac{\theta_0}{2}\, e^{-j\phi_0/2} \\ \sin\frac{\theta_0}{2}\, e^{+j\phi_0/2} & -\cos\frac{\theta_0}{2}\, e^{-j\phi_0/2} \end{bmatrix} \qquad S = \begin{bmatrix} \cos\frac{\theta_0}{2}\, e^{-j\phi_0/2} & \sin\frac{\theta_0}{2}\, e^{-j\phi_0/2} \\ \sin\frac{\theta_0}{2}\, e^{+j\phi_0/2} & -\cos\frac{\theta_0}{2}\, e^{+j\phi_0/2} \end{bmatrix}. \tag{20}$$

This permits us to make similarity transforms between the bases for operators:

$$D = \begin{bmatrix} \cos\theta_0 & \sin\theta_0\, e^{-j\phi_0} \\ \sin\theta_0\, e^{+j\phi_0} & -\cos\theta_0 \end{bmatrix} \qquad D_0 = \begin{bmatrix} 1 & 0 \\ 0 & -1 \end{bmatrix}$$

$$D \;=\; S\, D_0\, S^\dagger \qquad\qquad D_0 \;=\; S^\dagger\, D\, S\,. \tag{21}$$

In words, this says that D, operating on a vector in the conventional basis set, is equivalent to the operator D_0 operating in the eigenvector basis set. That is, if we are in the conventional basis we must first transform the vector's co-ordinates to the eigenbasis with $S^\dagger$, then operate on the result with D_0, the operator's representation in the eigenbasis, and finally use S to transform the resultant vector back to co-ordinates in the conventional basis. The reason we do this is to enable a simple integration of the coupled mode differential equation, Eqn (9).

Solution of the coupled mode equation

We can formally integrate the coupled mode equation, Eqn (17), as

$$\frac{d}{dz}\begin{bmatrix} a_1 \\ a_2 \end{bmatrix} = -j\bar{\kappa} D \begin{bmatrix} a_1 \\ a_2 \end{bmatrix} \Longrightarrow \begin{bmatrix} a_1(z) \\ a_2(z) \end{bmatrix} = e^{-j\int \bar{\kappa} D\, dz} \begin{bmatrix} a_1(0) \\ a_2(0) \end{bmatrix}, \tag{22}$$

as can be seen by substituting into the differential equation. We assume that the coupling does not vary along the length of the coupling region, so that

$$-j\int \bar{\kappa} D\, dz \;=\; -j\bar{\kappa} D z.$$

Then

$$\begin{bmatrix} a_1(z) \\ a_2(z) \end{bmatrix} = e^{-j\bar{\kappa} D z} \begin{bmatrix} a_1(0) \\ a_2(0) \end{bmatrix} = [\mathbf{I} + (-j\bar{\kappa} D z) + \frac{1}{2!}(-j\bar{\kappa} D z)^2 + ...] \begin{bmatrix} a_1(0) \\ a_2(0) \end{bmatrix}$$

$$= [\mathbf{I} + (-j\bar{\kappa} z S D_0 S^\dagger) + \frac{1}{2!}(-j\bar{\kappa} z S D_0 S^\dagger)^2 + ...] \begin{bmatrix} a_1(0) \\ a_2(0) \end{bmatrix}.$$

But since

$$(-j\bar{\kappa} z S D_0 S^\dagger)^n = (-j\bar{\kappa} z)^n\, (S D_0 S^\dagger)^n = (-j\bar{\kappa} z)^n (S D_0^n S^\dagger),$$

we have

$$\begin{bmatrix} a_1(z) \\ a_2(z) \end{bmatrix} = S\, [\mathbf{I} + (-j\bar{\kappa} z D_0) + \frac{1}{2!}(-j\bar{\kappa} z D_0)^2 + ...] S^\dagger \begin{bmatrix} a_1(0) \\ a_2(0) \end{bmatrix}.$$

Because D_0 is diagonal, D_0^n is also diagonal: $D_0^n = \begin{bmatrix} 1^n & 0 \\ 0 & (-1)^n \end{bmatrix}$. This simplifies the expression to

$$\begin{bmatrix} a_1(z) \\ a_2(z) \end{bmatrix} =$$

$$S \begin{bmatrix} 1 + (-j\bar{\kappa} z(+1)) + \frac{1}{2!}(-j\bar{\kappa} z(+1))^2 + ... & 0 \\ 0 & 1 + (-j\bar{\kappa} z(-1)) + \frac{1}{2!}(-j\bar{\kappa} z(-1))^2 + ... \end{bmatrix} S^\dagger \begin{bmatrix} a_1(0) \\ a_2(0) \end{bmatrix}$$

or

$$\begin{bmatrix} a_1(z) \\ a_2(z) \end{bmatrix} = S \begin{bmatrix} e^{-j\bar{\kappa}z} & 0 \\ 0 & e^{+j\bar{\kappa}z} \end{bmatrix} S^{\dagger} \begin{bmatrix} a_1(0) \\ a_2(0) \end{bmatrix}. \tag{23}$$

This equation exemplifies the spectral theorem [2, 11] from linear algebra. In words, it says that once the initial 2D state vector has been transformed to the eigenbasis by means of co-ordinate transformation $S^{\dagger}$, the top and bottom components are the amplitudes of that state vector in the slow and fast eigenstates, respectively. These amplitudes are not mixed, by virtue of the diagonal matrix, but are multiplied $e^{\mp j\bar{\kappa}z}$ as they propagate a distance z through the coupler. At the end of the propagation, the two components are co-ordinate transformed back to the original basis by S, to give the final output vector. Performing the matrix multiplication indicated in Eqn (23), one has the general solution for the ideal directional coupler:

$$\begin{bmatrix} a_1(z) \\ a_2(z) \end{bmatrix} = \begin{bmatrix} \cos\bar{\kappa}z - j\cos\theta_0 \sin\bar{\kappa}z & -je^{-j\phi_0}\sin\theta_0 \sin\bar{\kappa}z \\ -je^{+j\phi_0}\sin\theta_0 \sin\bar{\kappa}z & \cos\bar{\kappa}z + j\cos\theta_0 \sin\bar{\kappa}z \end{bmatrix} \begin{bmatrix} a_1(0) \\ a_2(0) \end{bmatrix}. \tag{24}$$

For the particular case of an ideal 3 dB coupler, we would have $\bar{\kappa}z = \pi/4$, $\theta_0 = \pi/2$, and $\phi_0 = 0$ which, for a coupler of length $z = L$, reduces Eqn (24) to

$$\begin{bmatrix} a_1(L) \\ a_2(L) \end{bmatrix} = \frac{1}{\sqrt{2}} \begin{bmatrix} 1 & -j \\ -j & 1 \end{bmatrix} \begin{bmatrix} a_1(0) \\ a_2(0) \end{bmatrix}. \tag{25}$$

Geometrical representation

General form

It can be shown [1] that our map for the vectors is equivalent to the statement that

$$\vec{s} = \langle s | \sigma_i \hat{e}_i | s \rangle \tag{26}$$

and that the equation of motion is

$$\frac{d\vec{s}}{dz} = 2\vec{\kappa} \times \vec{s}, \tag{27}$$

namely a precession of $\vec{s}$ about the vector $\vec{\kappa}$ at a rate of $2\kappa\ rad/m$.[2] This can be proven by differentiating Eqn (26), using Eqn (16), the equation of motion, as well as its adjoint, and applying the commutator relations for the σ_i [1, 2, 3, 12]. Here, we approach the problem from the geometrical direction.

Our derivation of the general coupler equation, Eqn (24), by way of Eqn (23), shows that, by construction, its eigenvalues are the diagonal elements $e^{\mp j\bar{\kappa}z}$, and the eigenvectors are $|s\rangle$ and $|f\rangle$, as given in Eqn (19). The matrix in brackets inside Eqn (23) is familiar from the discussion surrounding Eqn (12). There, we saw that such a diagonal form for the matrix was equivalent to rotation about the $\hat{\mathbf{e}}_3$ axis. In Eqn (23), however, we have a similarity transform: the diagonal matrix is sandwiched between S and $S^{\dagger}$. This means that the operator is not rotating about the $\hat{\mathbf{e}}_3$ axis, but is performing the "similar" operation in the new co-ordinate system defined by the similarity transform. In other words, the operator

$$S \begin{bmatrix} e^{-j\bar{\kappa}z} & 0 \\ 0 & e^{+j\bar{\kappa}z} \end{bmatrix} S^{\dagger} \tag{28}$$

performs, in the new basis, the operation "similar to" the operation performed by

$$\begin{bmatrix} e^{-j\bar{\kappa}z} & 0 \\ 0 & e^{+j\bar{\kappa}z} \end{bmatrix} \tag{29}$$

[2] In the telecommunications literature, it is customary to suppress the factor of 2 in this equation by dividing terms in the 2×2 matrices by 2 [2, 3, 12].

in the original basis. That is, in the co-ordinate system defined by $S^{\dagger}$, namely $|s\rangle \rightarrow |1\rangle \sim \hat{\mathbf{e}}_3$, the operator in Eqn (28) creates a rotation about the vector $\vec{s}$ with angular velocity 2κ, just as the operator in Eqn (29) does about the $\hat{\mathbf{e}}_3$. Thus, Eqns (23,24) in the 2D space describe, in the geometric representation, a uniform rotation (i.e. at constant rate as z increases) about the unit vector corresponding to the eigenstate of Eqn (16), namely $\hat{\kappa}$. Indeed, this is the same form we have discussed in the context of polarization optics in

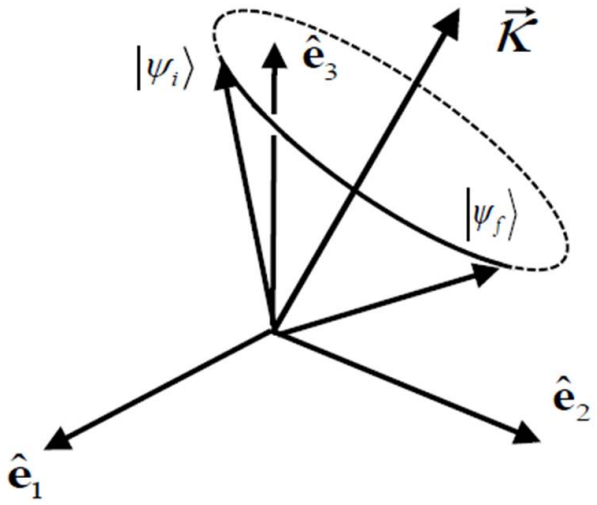

Fig. 11: Coupler evolution: general case. Initial state $|\psi_i\rangle$ evolves into state $|\psi_f\rangle$ under the influence of coupler operator $\vec{\kappa}$.

earlier work [2, 3].

The general geometric solution of the coupler equation is shown in Fig. 11. The components of $\vec{\kappa}$, found either by the components in Eqn (9) or by knowledge of the eigenstate angles θ_0 and ϕ_0 in Eqns (20, 21), create the vector about which a typical vector $\vec{s}$ (representing a normalized input state to the coupler, in our normal form) rotates. The magnitude of the rotation (i.e. the angle about $\vec{\kappa}$ through which the trajectory from $|\psi_i\rangle$ to $|\psi_f\rangle$ passes) is $2\bar{\kappa}z$. The rotation does not change the amplitude of $\vec{s}$, in the same way that Eqn (24), a unitary matrix, doesn't change the magnitude of the 2D vector. A more general form, including an overall phase constant, was treated earlier [2, 3] to be able to incorporate the overall propagation constant and topological phase, which we have suppressed in this report. That approach entails "fiducial paddles" which track the overall phase of the state, necessary when dealing with interferometric problems. It includes a more graceful way of handling the branch cut discussed above.

Features of the geometric representation

Several features of coupling which are not immediately clear in the 2D representation cam be gleaned from viewing Fig. 11.

First, recall that the basis set we are using, $\pm\hat{\mathbf{e}}_3$, are the ports or waveguides for the coupler. If one of them is "slow" we conventionally define it as $+\hat{\mathbf{e}}_3$. Then, by virtue of normal form Eqn (10), the input to the coupler is defined by *both* the relative amplitudes between the two guides and the phase between those two optical components. For light introduced into one guide only, $|\psi_i\rangle$ is $\pm\hat{\mathbf{e}}_3$.

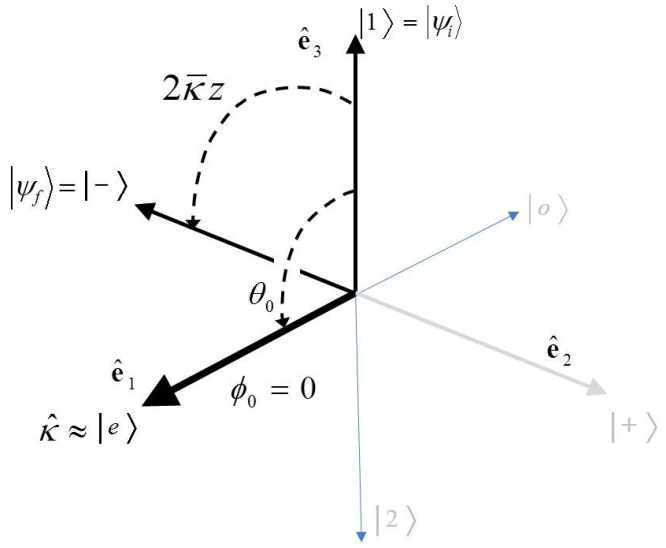

Fig. 12: Coupler evolution: ideal 3 dB coupler. Initial state $|\psi_i\rangle = |1\rangle$ evolves into final state $|\psi_f\rangle$. Vector for coupler operator is along $\hat{\mathbf{e}}_1$ axis, and creates a rotation of $2\bar{\kappa}z = \pi/2$.

Second, in the geometric approach, there is no clear distinction between "coupling strength" as defined by κ_1, κ_2 (Eqn (9)'s "off-diagonal" components) and "detuning" as defined by κ_3, a measure of the difference between the guides' propagation constants in Eqn (5). That is, three κ_i are components of the single vector $\vec{\kappa}$.

This gives rise to the third point: there is a definite interplay between the coupling strength and the detuning. Namely, if the detuning κ_3 is much greater than the coupling strength's magnitude $\sqrt{\kappa_1^2 + \kappa_2^2}$, then it is impossible to attain 3 dB coupling. Indeed, if $\theta_0 < \pi/4$, the circle about $\vec{\kappa}$ on which $\hat{\mathbf{e}}_3$ resides can not reach the $\hat{\mathbf{e}}_1 - \hat{\mathbf{e}}_2$ plane. Since points on this plane are at angle $\theta = \pi/2$, it is these points (more accurately, points on the "equator" of Fig. 11) that have equal powers in the two guides. This fact is more difficult to tease out of the 2D form Eqn (24) than the geometric form. It is apparent more detuning must be compensated by more coupling to retain even power splitting. In fact, one can see that a more robust 3 dB coupler design might be to intentionally detune the coupler so that the arc finishes tangentially to the $\hat{\mathbf{e}}_1 - \hat{\mathbf{e}}_2$ plane.

Fourth, one sees that complete transfer of power is only possible if (i) $\kappa_3 = 0$, i.e. the coupler has no detuning, and (ii) $2\kappa z = \pi/2$. Again, this is obvious from the geometric picture, but requires more digging in the 2D representation.

Finally, Fig. 12 shows the typical situation for an ideal 3 dB coupler used as a power splitter. The basis states are the two uncoupled guide states, $|1\rangle$ and $|2\rangle$. In the ideal case, the guides are identical, so $\kappa_3 = 0$: thus $\vec{\kappa}$ lies in the $\hat{\mathbf{e}}_1 - \hat{\mathbf{e}}_2$ plane. Specifically, in the ideal case, only $\kappa_1 \neq 0$, so $\vec{\kappa}$ lies along the $\hat{\mathbf{e}}_1$ direction. When light is introduced into one of the guides, say $|1\rangle$, it evolves as it propagates through the coupler, rotating about $\vec{\kappa}$. To evenly split the light between the two guides, rotation $2\kappa z$ for the coupler's length z is $\pi/2$: at this point, $|\psi_f\rangle$, the final state is $\pi/2$ from both $|1\rangle$ and $|2\rangle$, so the amplitude in each guide is $cos\,\frac{\pi/2}{2} = \frac{1}{\sqrt{2}}$. There is a differential phase shift of $\pi/2$ that is acquired in traversing the coupler: this is evident from looking at Fig 8 and from Eqn (24). If this coupler were part of an interferometer, we would have to add the phases we suppressed in the gauge transformation, as well. Earlier maps (Fig 3) show how

the relative phases arise in the various output states.

Connection to conventional eigenstate analysis

For completeness, we include a view of coupled waves by analyzing it using the conventional eigensystem method. The general form for the coupled waves, Eqn (9), must have the form

$$\frac{d}{dz}\begin{bmatrix} a_1 \\ a_2 \end{bmatrix} = -j\begin{bmatrix} \kappa_3 & \kappa_1 - j\kappa_2 \\ \kappa_1 + j\kappa_2 & -\kappa_3 \end{bmatrix}\begin{bmatrix} a_1 \\ a_2 \end{bmatrix} = -jk\begin{bmatrix} a_1 \\ a_2 \end{bmatrix} \tag{30}$$

for the eigenvalues k: the left half describes the equation of motion, and the right half describes the oscillatory form necessary for normal modes. When the right half of this eigenvalue equation is solved, we find the eigenvalues

$$k = \pm\bar{\kappa} = \pm\sqrt{\kappa_1^2 + \kappa_2^2 + \kappa_3^2},$$

as we would expect from the discussion above. Recalling Eqn (7), the slowly varying transformation, Eqn (30) implies that there are two allowed solutions for the propagation constant, $\bar{k} \pm \kappa$, for a field introduced at frequency ω. This is conventionally displayed on a dispersion curve such as Fig 13.

The basic features of the dispersion curve are shown in the inset, which is most easily interpreted by considering the wavenumbers k, on the horizontal axis, to be dependent on the optical frequency ω, on the vertical axis. We have been discussing the case for a single optical frequency, represented by a horizontal line on this plot. The dashed lines represent the *uncoupled* wavenumbers for the two waveguides as a function of ω, shown as distinct in this figure, for generality. At the "phase-matched" frequency, ω_0, the two uncoupled guides have the same wavenumber, k_0. Since the phase velocity is $v_p = \omega/k$, the uncoupled guides have the same phase velocity at ω_0, but it is clear that they have different group velocities, $v_g = \partial\omega/\partial k$, since the dashed lines have different slopes. The solutions to the eigenvalue equation are $k_\pm = \bar{k} \pm \bar{\kappa}$, and are shown as the solid lines. It is clear that k_- is always less than the minimum of k_1, k_2, while k_+ is greater. Thus, k_+, for instance, is the "slower" of the modes, and the $k_\pm$ approach the uncoupled values for large values of detuning $\omega - \omega_0$. (In this simplification of a dispersion relation, the two modes have constant group velocities, but their phase velocities change with frequency.)

A deeper view of the dispersion curve is shown in the larger detail of Fig 13, a blow-up of the region around the phase-matched point. For generality, we choose a non-zero detuning: the horizontal line is for $\omega > \omega_0$. The four dots are the intersection of ω and the dispersion curves, with the abscissae corresponding to the coupled (k_-, k_+) and uncoupled (k_1, k_2) wavenumbers. It is clear that the coupled wavenumbers are farther from the mean $\bar{k}$ than the uncoupled wavenumbers, a general "splitting" feature of perturbation analyses.

Point a) on the diagram shows the splitting of the wavenumbers for the case of zero detuning. In this view, the magnitude of the splitting is the coupling strength, $\sqrt{\kappa_1^2 + \kappa_2^2}$: it corresponds to the largest deviation $k_\pm$ has from uncoupled $k's$. For the more general case of non-zero detuning, the uncoupled wavenumbers separate because the slopes of the dashed curves correspond to different $v_g = \partial\omega/\partial k$. The amount of the splitting is given by Eqn (5) and has the geometric representation shown at point b) in the figure: since

$$v_{g\,i} \equiv \frac{\partial\omega}{\partial k} = \frac{\omega - \omega_0}{k_i - k_0},$$

the uncoupled mode splitting is related to the detuning and group velocities by

$$2\kappa_3 = (\omega - \omega_0)(v_{g1}^{-1} - v_{g2}^{-1}).$$

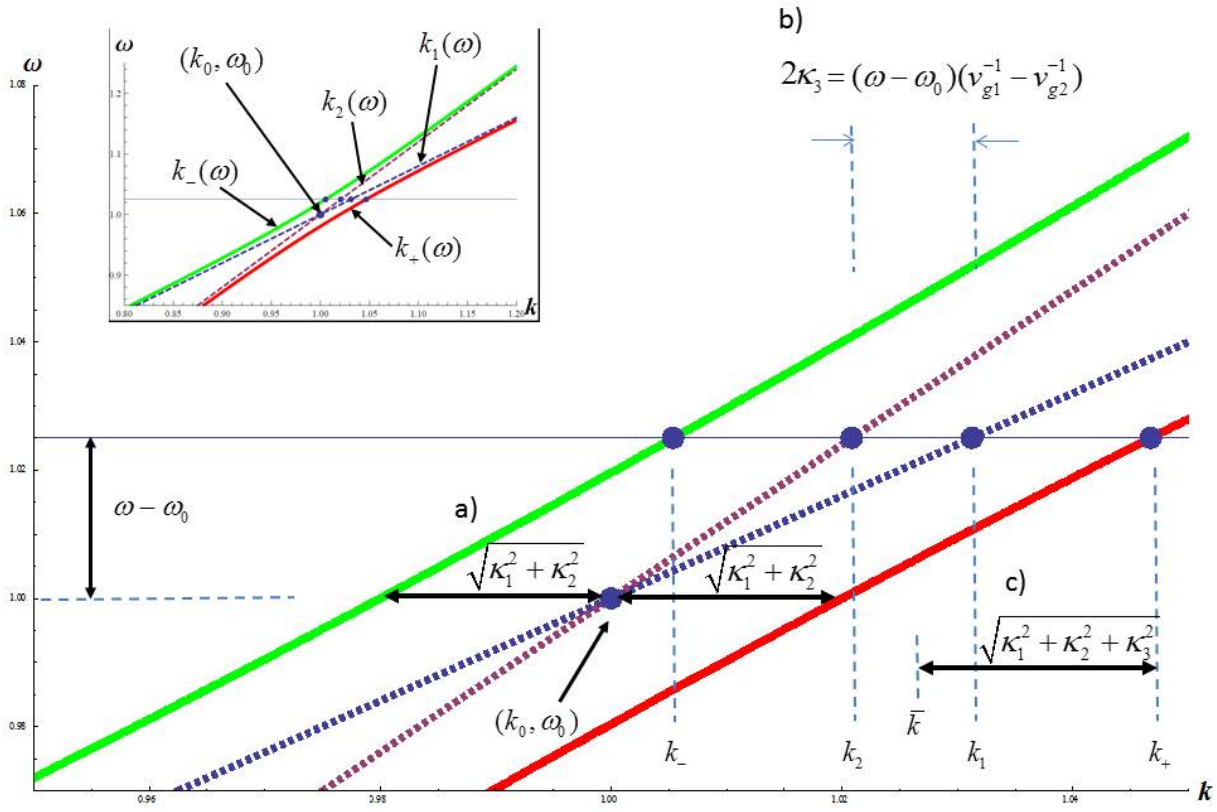

Fig. 13: Coupler dispersion curve. Inset: Plot of uncoupled guide dispersion curves(dashed) distorting in the presence of waveguide coupling (solid). Detail: The deviation of the coupled curves is the rss deviation in k due to detuning of the uncoupled modes (κ_3, which increases linearly with $\Delta\omega$), and the idealized "coupling strength" $\sqrt{\kappa_1^2 + \kappa_2^2}$ at zero detuning. The rss deviation of these two contributions is the deviation of the coupled propagation constants from the average propagation constant, $\bar{k}$.

Then the deviation of the coupled wavenumbers from the mean $\bar{k}$ is the root-summed-square (rss) of the coupling and detuning deviations, namely $\kappa = \sqrt{\kappa_1^2 + \kappa_2^2 + \kappa_3^2}$ as shown at point c) in the figure. This shows why the deviation is the coupling strength for zero detuning, while for large detuning it tends to the detuning itself.

In contrast, one sees in the geometric view of Fig 11 a visual way of describing the same facts. In this view

- The splitting is due to the length of the vector $\vec{\kappa}$, since one could transform to that basis set.
- Magnitude $|\vec{\kappa}|$ is determined by the detuning (component in the $\hat{\mathbf{e}}_3$ direction) and the coupling strength (components in the $\hat{\mathbf{e}}_1 - \hat{\mathbf{e}}_2$ plane)
- That magnitude is found by the Pythagorean theorem and is why the detuning and coupling are combined as a root-summed-square

- The zero detuning limit reflects that the κ_3 component is zero, so the magnitude $|\vec{\kappa}|$ is determined only by the coupling components
- The large detuning limit reflects the fact that the $|\vec{\kappa}| \rightarrow \kappa_3$ if $\kappa_3 >> \kappa_1, \kappa_2$.
- Not only is there a description of the eigenvalues, the coupler's component evolution, magnitude and phase, is described in the same view.

VII SUMMARY

In this report, we have used the directional coupler as a model for coupled mode theory. We have

- shown how the fast phase variations in the mode can be transformed away to yield the standard coupled mode equations,
- used a phasor approach throughout to physically motivate the coupling processes,
- shown how the phase ambiguity in the geometrical approach can be resolved,
- demonstrated how the phases are related in co-ordinate transformations,
- used a similarity transform analysis to provide an alternate derivation of the coupling equation, and
- established connections between the conventional dispersion maps for waveguides and the geometrical representation of coupled waves.

VIII REFERENCES

[1] N.J. Frigo, "A generalized geometrical representation of coupled mode theory," *IEEE J. Quant. Electron.*, vol. QE-22 (11), pp. 2131-2139, 1986.

[2] N.J. Frigo and F. Bucholtz, "Geometrical representation of optical propagation phase," *J. Lightwave Tech.*, vol. 27 (15), pp. 3283- 3293, Aug. 2009.

[3] N.J. Frigo, F. Bucholtz, and C.V. McLaughlin, "Polarization in phase modulated optical links: Jones- and generalized Stokes-space analysis," *J. Lightwave Tech.*, vol. 31 (9), pp. 1503-1511 (2013).

[4] J.N. Damask, *Polarization optics in telecommunications*, New York, NY: Springer, 2004.

[5] J.R. Pierce, "Coupling of modes of propagation," *J. Appl. Phys.*, vol. 25, pp.179-183 (1954).

[6] A. Yariv, "Coupled-mode theory for guided-wave optics," IEEE. J. Quantum Elect., vol. QE-9, pp.919-933 (1973).

[7] H.A. Haus, *Waves and Fields in Optoelectronics*, Prentice-Hall, Englewood Cliffs, New Jersey, 1984.

[8] R.P. Feynman, F.L. Vernon, and R.W. Hellwarth, "Geometrical representation of the Schrodinger equation for solving maser problems," *J. Appl. Phys*, vol. 28, pp. 49-52 (1957).

[9] D. Goldstein, *Polarized Light*, New York, NY: CRC Press, 2003.

[10] C.W. Barnes, "Conservative coupling between modes of propagation – a tabular summary," *Proc. IEEE*, vol. 52, pp. 64-73 (1964).

[11] K. Hoffman and R. Kunze, *Linear Algebra*, 2nd ed., Englewood Cliffs, nJ: Prentice-Hall, 1971.

[12] J.P. Gordon and H. Kogelnik, "PMD fundamentals: polarization mode dispersion in optical fibers," *Proc. Nat. Acad. Sci.*, vol. 97, pp. 4541-4550 (2002).